See related Commentary on page 1072

The American Journal of Pathology, Vol. 176, No. 3, March 2010

DOI: 10.2353/ajpath.2010.090648

Epithelial and Mesenchymal Cell Biology

Epithelial-Stromal Interaction 1 (EPSTI1) Substitutes for Peritumoral Fibroblasts in the Tumor Microenvironment

Michala de Neergaard,* Jiyoung Kim,* René Villadsen,* Agla J. Fridriksdottir,* Fritz Rank,† Vera Timmermans-Wielenga,† Anita Langerød,‡ Anne-Lise Børresen-Dale,‡ Ole W. Petersen,* and Lone Rønnov-Jessen§

From the Departments of Cellular and Molecular Medicine, Faculty of Health Sciences, University of Copenhagen, Copenhagen N, Denmark; the Department of Pathology,† State University Hospital, Rigshospitalet, Copenhagen, Denmark; the Department of Genetics,‡ Institute for Cancer Research, Norwegian Radium Hospital, Oslo University Hospital, Oslo, Norway; and Cell and Developmental Biology, Department of Biology,§ University of Copenhagen, Copenhagen, Denmark*

Tumor cells can activate stroma, yet the implication of this activation in terms of reciprocal induction of gene expression in tumor cells is poorly understood. *Epithelial Stromal Interaction 1* (*EPSTI1*) is an interferon response gene originally isolated from heterotypic recombinant cultures of human breast cancer cells and activated breast myofibroblasts. Here we describe the first immunolocalization of EPSTI1 in normal and cancerous breast tissue, and we provide evidence for a role of this molecule in the regulation of tumor cell properties and epithelial-mesenchymal transition. In general, no EPSTI1 staining was observed in normal breast epithelial cells from reduction mammoplasties (n = 25). However, in carcinomas, staining was positive in 22 of 40 biopsies and inversely correlated with the level of differentiation. To address the function *of EPSTI1*, we expressed *EPSTI1* ectopically in one cell line and silenced endogenous *EPSTI1* by RNA interference in another. Irrespective of the experimental approach, *EPSTI1* expression led to an increase in tumorsphere formation—a property associated with breast stem/progenitor cells. Most remarkably, we show that EPSTI1, by conveying spread of tumor cells, can replace peritumoral activated fibroblasts in a tumor environment assay. These observations implicate *EPSTI1* as a hitherto unappreciated regulator of tumor cell properties. ***(Am J Pathol 2010, 176:1229–1240; DOI: 10.2353/ajpath.2010.090648)***

Solid tumors are composed of neoplastic epithelial cells and non-neoplastic fibroblasts, blood vessels, macrophages, and immune cells embedded in a collagenous extracellular matrix collectively often referred to as the peritumoral stroma (for a recent review see[1]). The most dramatic consequence of epithelial neoplasia within the peritumoral stroma is the accumulation of so-called activated fibroblasts or myofibroblasts.[2,3] Myofibroblasts can be recruited from resident fibroblasts by the action of transforming growth factor-β secreted by tumor cells or macrophages in a paracrine manner.[3] Evidence is accumulating that myofibroblasts participate actively in tumor formation and progression. They have been shown to secrete a variety of factors such as stromal derived factor 1,[4] migration stimulating factor,[5] hepatocyte growth factor (HGF[6]), and urokinase (uPA[7]), which function either directly on tumor cells via specific receptors such as CXCR4, cMet, and uPAR[4,6,7] or indirectly via, eg, inflammatory cells, to generate a more tumor-prone microenvironment.[8]

One of the consequences of tumor cell-fibroblast interaction at the functional level is spread of carcinoma cells and invasion of collagen lattices.[3,6,9] The functional

Supported by the Danish Cancer Society; Dansk Kræftforskningsfond; Danish Research Counsil; Fru Astrid Thaysens Legat for Lægevidenskabelig Grundforskning; LEO Pharma Forskningsfond; the Toyota Foundation; EuroCSC contract no: 037632; the Lundbeck Foundation; the Novo Nordic Foundation; the Danish Research Agency, contract no. 2107-05-0006; DAN-ED; NIH, contract no. R01CA064786; the Friis Foundation and the Simon Spies Foundation.

Accepted for publication October 29, 2009.

The use of human material has been reviewed by the Regional Scientific Ethical Committees for Copenhagen and Frederiksberg and approved with reference to (KF)(11) 263995. Animal experiments were conducted in accordance with procedures approved by the Animal Experiments Inspectorate.

Address reprint requests to Lone Rønnov-Jessen, Associate Professor, D.Sc., Department of Biology, Universitetsparken 13, DK-2100 Copenhagen Ø, Denmark. E-mail: lronnov-jessen@bio.ku.dk.

equivalent to this behavior in tissue culture plastic is scattering, and this is mediated by HGF both within collagen gel and in monolayer culture.[9–11] At the molecular level, cell scattering is associated with various degrees of epithelial-mesenchymal transition (EMT).[12] This includes loss of one or more epithelial cell–cell contacts and gain of a partial mesenchymal differentiation program along with an increase in cellular motility.[13] Although originally an embryonic concept, EMT has been adopted by cancer biologists to describe loss of epithelial differentiation and tumor cell spread (for review see[14]). Another, albeit more recent, property of some solid tumors including breast cancer is that of rare cancer-initiating cells or cancer stem cells (CSCs) fuelling the bulk of the tumor. Intriguingly, several lines of evidence suggest that CSCs share properties in common with EMT cells.[15,16] Thus, CSCs are most prominent in a relatively rare subset of basal-like breast cancers referred to as metaplastic or the "claudin-low" because they contain a large proportion of EMT-like spindle cells, which are low in expression of an epithelial cell–cell contact program.[17] More specifically, induction of EMT in human mammary epithelial cells results in expression of stem cell markers and increased ability to form mammospheres, and conversely, stem cells isolated from either the normal breast or breast cancer express EMT markers.[15]

We originally discovered *Epithelial-Stromal Interaction 1* (*breast*; *EPSTI1*) by comparing the transcriptional profile of cocultured breast cancer cells and stromal fibroblasts with the collective profile of the two cell types cultured in separate.[18] *EPSTI1* was expressed in all breast cancers tested with little expression in the normal breast. Subsequently, it has been shown that *EPSTI1* is one of the most highly expressed genes in a unique set of interferon (IFN) response genes.[19] Most recently, characterization of tumor cell–fibroblast interaction effects in cocultures deconvoluted a complex picture of global gene expression profiles in breast cancer, the most prominent of which was an interferon response signature including *EPSTI1*.[20] Tumors expressing this signature were associated with significantly shorter overall patient survival.[20]

Given the potential importance of stroma in stem cell niches and in tumor progression, it is essential to explore genes that are submitted to regulation by stroma in cancer cells. Here we undertook to provide the first immunocytochemical staining of EPSTI1 in breast cancer and the first functional characterization of this prominent interferon response gene. We show that EPSTI1 is a nucleocytoplasmic protein expressed most widely in breast cancer subtypes exhibiting a poor prognosis, and that its expression may substitute for activated peritumoral fibroblasts in the microenvironment.

Materials and Methods

Establishment of an EPSTI1-Transduced Cell Line

The coding region of *EPSTI1* was tagged with the FLAG epitope in the C terminus by PCR amplification using forward and reverse primers, 5′-CGGTCGACGCCACCATGAACACCCGCAATAGA-3′ and 5′-CCATCGATGGTCACTTGTCATCGTCGTCCTTGTAGTCTATACCCCAGCTGTTACC-3′, cloned into the pRevTRE vector (Clontech, BD Biosciences, Brøndby, Denmark) at *cla I* and *sal I* restriction sites, and transduced into MCF-7 Tet-Off cells using the RetroMax retroviral transduction assay as described by the manufacturer (Imgenex, Nordic BioSite, Copenhagen, DK). Infected cells containing the pRevTRE-FLAG-*EPSTI1* vector were selected by adding 400 μg/ml hygromycin B (Gibco BRL, Invitrogen, Tåstrup, DK).

Cell Culture

MCF-7–EPSTI1–Tet-off cells were cultured in DMEM 1885 (Gibco BRL, Invitrogen) with 5% Tet System Approved fetal bovine serum (FBS, Clontech, Medinova, Glostrup, DK), 2 mmol/L L-glutamine, 100 μg/ml G418 sulfate, and 100 μg/ml hygromycin B (Invitrogen). Expression was turned off with 100 ng/ml doxycycline hydrochloride (Dox; Sigma-Aldrich, Brøndby, DK). MDA-MB-231 cells (European Collection of Cell Cultures, Sigma-Aldrich), hTERT immortalized human breast fibroblasts (kindly provided by Dr. C. Eaves, Terry Fox Research Laboratory, British Columbia Cancer Agency, Vancouver, British Columbia, Canada), and human normal breast fibroblasts[21] were cultured in DMEM/F12 (1:1, Gibco, Invitrogen) with 5% FBS (Gibco) and 2 mmol/L L-glutamine. Parent MCF-7 cells were cultured as described.[22] For monolayer coculture experiments hTERT immortalized fibroblasts were plated at a density of $4.8 \times 10^5/cm^2$ with or without $8 \times 10^3/cm^2$ MCF-7 cells and analyzed for EPSTI1 expression after four days. A cell line with stem cell properties (D492) was cultured in H14 as described.[23] IFN-α (Chemicon, Millipore) was added to a final concentration of 1000 U/ml at the indicated time periods. All cells were cultured at 37°C in a humidified incubator with 5% CO_2.

RNAi-Mediated Suppression of EPSTI1 Expression

Of three Stealth RNAi duplexes without overhanging at the 3′ from Invitrogen, one (EPSTI1-HSS150784; sense 5′-GAGCAAUCUGGAGGCUGUUGGAAUA-3′ and antisense 5′-UAUUCCAACAGCCUCCAGAUUGCUC-3′, here EPSTI1-siRNA2) targeting 947-971 of the originally published sequence,[18] efficiently interfered with EPSTI1 expression in MCF-7–EPSTI1–Tet-off cells. We designed three other Stealth RNAi duplexes, of which one (sense 5′-AGUCAACCAGGUGGCCUCGAGCAAU-3′ and antisense 5′-AUUGCUCGAGGCCACCUGGUUGACU-3′) partly overlapped EPSTI1-siRNA2 by targeting 929-953, and thus validated the specificity of EPSTI1-siRNA2. The other two (EPSTI1-siRNA1; sense 5′-CAUUUAGAGAGCAUCAGCUUUACAA-3′ and antisense 5′- UUGUAUUGCUGAUGCUCUCUAAAUG-3′ and EPSTI1-siRNA3: sense 5′-GACUGAACACUGGAGGGUAAAUAAU-3′ and antisense 5′-AUUAUUUACCCUCCUGUGUUCAGUC-3′) targeted 618-642 and 877-901, respectively. A BLAST search ensured specific *EPSTI1* targeting. Negative controls in-

cluded siRNA with low CG content (cat. no. 12935-200, control-siRNA1) and siRNA with medium CG content (cat. no. 12935-300, Invitrogen, control-siRNA2).

To optimize the transfection protocol, BLOCK-iT Fluorescent Oligo (Invitrogen) was used. MDA-MB-231 cells at a density of 2×10^4 cells/cm^2 and D492 at a density of 2.8×10^4 cells/cm^2 were cultured up to 48 hours before transfection using Lipofectamine™2000 (Invitrogen) with Stealth RNA duplexes at a final concentration of 200 nmol/L. Up to 48 hours later, the culture medium was changed with or without IFN-α, and cells were further analyzed after the indicated time periods.

shRNA-Mediated Suppression of EPSTI1 Expression and Xenografts

For shRNA suppression of EPSTI1, a specific shRNAmir expressed in the pGIPZ lentiviral vector from Open Biosystems (shEPSTI1; clone Id: V2LHS_160196) was used. A non-silencing-GIPZ lentiviral shRNAmir construct (shControl, cat. No. RHS4346) was used as negative control. The pGIPZ vector contained a puromycine selectable marker and turbo green fluorescent protein, GFP.

Lentiviruses were generated in 293 FT cells (from Invitrogen) by cotransfecting either shEPSTI1 or shControl with second generation packaging plasmids (pVSVG, pCMV, PAX8) using Arrest-In transfection reagent (Open Biosystems, Thermo Scientific, Hillerød, DK) according to the manufacturer's protocol.

Virus containing media were harvested 48 hours post transfection, followed by low spinning (3000 rpm for 2 minutes), filtering through a 0.45 μm filter, and concentrating at 40,000 rpm for 20 minutes. MDA-MD-231 cells were transduced by overnight incubation in virus containing media with polybrene (8 μg/ml, Sigma). After 48 hours, transfected cells were selected by puromycine (5 μg/ml, Sigma). Successful transfection was confirmed by visual inspection of the presence of GFP in the fluorescence microscope. Suppression of induction by shEPSTI1 on IFN-α exposure was further confirmed by real-time PCR (see below), which revealed a 20-fold reduction of *EPSTI1* expression in shEPSTI1 versus shControl.

The influence of EPSTI1 on tumor initiation was determined by assessing tumorigenicity in 7-week-old NOD/SCID mice (NOD.Cg-Prkdcscid Il2rgtm1Wjl/SzJ, Jackson Laboratories) housed in pathogen-free rodent facilities on sterilized ventilated racks and supplied with commercial chow and sterilized water. shEPSTI1 and shControl MDA-MB-231 cells were exposed to IFN-α for 15 hours before subcutaneous inoculation in both sides at the fourth mammary gland with 5×10^6, 5×10^5, or 5×10^4 cells, respectively. Mice were examined for tumor take once a week for six weeks, and then terminated and examined.

Reverse Transcriptase PCR

Total RNA was isolated using TRIzol Reagent (Invitrogen), treated with DNase (Fermentas, Germany), and EPSTI1 transcripts were amplified using 5′-TGAACACCCGCAATAGAGTG-3′ and 5′-GCTGCCGTTTCAGTTCCAGT-3′ primers and Expand™ High Fidelity PCR System at 94°C for 4 minutes, 40 cycles at 94°C for 1 minute, 60°C for 1 minute, 72°C for 1 minute, followed by 72°C for 7 minutes and hold at 4°C. GAPDH transcripts were amplified using 5′-ACCCACTCCTCCACCTTTG-3′ and 5′-CTCTTGTGCTCTTGCTGGG-3′ primers at 94°C for 2 minutes, 25 cycles at 94°C for 1 minute, 54°C for 1 minute, 72°C for 1 minute, followed by 72°C for 7 minutes and hold at 4°C. PCR products were analyzed by electrophoresis on agarose gels, and DNA ladders (Promega, Birkerød, DK) confirmed their sizes.

Protein Extraction

Cells were lysed in 20 mmol/L MOPS, 1 mmol/L EDTA, 150 mmol/L NaCl, 0.1% SDS, 1% NP-40, 1% sodium deoxycholate and protease inhibitor cocktail 1:100 (Sigma-Aldrich), and total protein concentration was determined with Bio-Rad DC Protein Assay (Bio-Rad, Copenhagen, DK).

Western Blotting

50 μg total protein was separated by SDS-PAGE on a 12% gel and transferred to Amersham Hybond-P polyvinylidene difluoride membrane (PVDF; GE Health care) with a molecular weight marker. The membrane was incubated with primary antibodies overnight at 4°C (anti-EPSTI1 3G7, 1:1000, Abnova, Taipei, Taiwan and anti–β-actin, clone AC-15, 1:1,000,000, Sigma-Aldrich), followed by incubation with the appropriate horseradish peroxidase-conjugated secondary antibody (Dako, Glostrup, DK) for one hour at room temperature. Signals were detected using Immobilon Western HRP Substrate (Millipore, Copenhagen, DK) and an AutoChemi system darkroom (UVP).

Immunocytochemistry and -Histochemistry

Normal breast ($n = 25$) and breast carcinoma biopsies ($n = 40$) were obtained from patients undergoing reduction mammoplasty for cosmetic reasons and surgical treatment for invasive breast cancer, respectively. Cultures and sections were fixed for 5 minutes in 3.7% formaldehyde (Merck, Darmstadt, Germany) in PBS, followed by 5 minutes in ice-cold methanol:acetone (1:1) at −20°C, and 2 × 7 minutes in 0.1% Triton X-100 (Sigma-Aldrich) in PBS with washes in PBS in between. Nonspecific binding was blocked with 10% normal goat serum (Biological Industries, Invitra, Fredensborg, DK) in PBS for 10 minutes. Primary antibodies were diluted in blocking buffer and incubated at room temperature for one hour followed by incubation with UltraVision ONE HRP Polymer (Lab Vision, Thermo Scientific) for 30 minutes or isotype specific secondary antibodies (Molecular Probes, Invitrogen). After washing, the immune reaction (with Ultravision ONE HRP Polymer) was visualized with 0.5 mg/ml 3,3′-Diaminobenzidine (DAB, Sigma-Aldrich) with 0.02% H_2O_2. Nuclei were counterstained with hematoxylin (Sigma-Aldrich) or TO-PRO-3 iodide (Invitrogen) 1:500 in PBS. Primary antibodies included anti-$\alpha 2\beta 1$-integrin (clone BHA2.1, 1:50, Millipore); anti-CAM5.2 recognizing cytokeratins 7/8 (clone CAM5.2, 1:2, BD Bio-

sciences); anti–claudin-1 (polyclonal, 1:40, Thermo Fisher Scientific); anti-EPSTI1 (clone 3G7, 1:200 for peroxidase and 1:40 for fluorescence [1:1000 for MCF-7-EPSTI1-Tet-off cells], Abnova); anti-fibronectin (clone FN-3E2, 1:40, Sigma-Aldrich); anti-cytokeratin 5 (polyclonal, 1:250, Covance, Nordic, BioSite); anti-ΔNp63 (polyclonal, 1:25, BioLegend, Nordic, BioSite), anti-PgR (clone SP2, 1:25, Thermo Fisher Scientific), anti–Ki-67 (SP6, 1:25, Thermo Fisher Scientific), anti-cytokeratin 14 (LL002, 1:25, Novocastra, Leica Microsystems, Herlev, DK), and anti–cytokeratin 19 (A53-B/A2, 1:50, Serotec, Oxford, UK). In addition to clone 3G7, four monoclonal (2A8, 6F9 [Abnova], ZZ4 [Santa Cruz, Heidelberg, Germany], custom monoclonal [AntibodyShop]) antibodies and two polyclonal (custom polyclonal (ImmunoVision) and A01 (mouse polyclonal, Abnova) antibodies were tested. None of these met our criteria for specificity in Western blotting and immunohisto-/cytochemistry.

Paraffin-embedded tissue arrays (33 types of human normal tissue, 96 human breast cancer tissue samples, Pantomics) were dewaxed and antigen retrieved with 10 mmol/L citrate buffer, pH 6.0, 15 minutes in a microwave oven and cooling for 20 minutes. Unspecific binding was blocked for 30 minutes in 10% goat serum before incubation with EPSTI1 antibody (clone 3G7 1:800) overnight at 4°C. Staining was visualized with Ultravision ONE HRP Polymer (Lab Vision) for 30 minutes.

Migration Assay

MCF-7–EPSTI1–Tet-off cells cultured with or without doxycycline for four days were plated in 12 wells with 8-μm pore size inserts (Becton Dickenson) in triplicate (1.5×10^5 cells per insert) and allowed to migrate for 24 hours. Cells on the upper side of the insert were scraped off, and migrated cells were stained with crystal violet. Stealth RNAi duplex transfected MDA–MB-231 were exposed to IFN-α for 15 hours before plating in inserts in triplicate (3×10^5 cells per insert), and allowed to migrate for 5.5 hours before staining. Migration was quantified using an ocular grid (×25). The morphology and integrin expression pattern during the migratory process was analyzed by phase contrast microscopy, immunocytochemistry, and FACS three to four hours after plating.

Tumor Environment Assay

Collagen gels (PureCol., Nutacon, Leimuiden, the Netherlands, final concentration of 2.4 mg/ml) were prepared as 0.5 ml gels in 24-well dishes as described[3,22] with 5×10^4 parent MCF-7 cells with or without 5×10^4 human breast fibroblasts[22] or 5×10^4 MCF-7–EPSTI1–Tet-off cells with or without 5×10^4 hTERT immortalized human breast fibroblasts in the presence or absence of doxycycline. To determine whether siRNAs could abrogate the interaction, parent MCF-7 cells were treated with EPSTI1-siRNA2 or control-siRNA2 for two days before confrontation with fibroblasts in 3-D gels. 10^{-10} mol/L estradiol (Sigma-Aldrich) and 10 ng/ml HGF (human recombinant protein; abcam) were included. The presence of estradiol was essential for tumor colony spread, whereas HGF did not augment the response further. Experiments were performed in triplicate, and the number of colonies exhibiting morphogenic behavior was quantified at day 7 to 8 using an ocular grid (×10, 3×50 colonies counted per gel using an ocular grid). Colonies were scored as spread if deviating from the spherical structure usually formed by MCF-7 cells when cultured alone in 3-D collagen gel.[22]

Mammosphere/Tumorsphere Assay

Cells were trypsinized, filtered through a 20-μm filter (BD Biosciences), 1 μg/ml propidium iodide (Molecular Probes, Invitrogen) was added, and live cells single cell sorted with a BD FACSAria cell sorter (BD Biosciences) into 96-well Ultra-Low Attachment Plates (Corning, Sigma-Aldrich) as described,[24] and the number of wells with one cell was determined. D492 and MDA-MB-231 were supplemented with IFN-α. The number of spheres was counted after 7 to 8 days.

Soft Agar Assay

Cells were suspended as 5×10^3 cells per 6-well in 1.5 ml 0.35% agar (Low melting agarose; Gibco) with appropriate medium on top of a bottom agar (1.5 ml 0.5% agar). 1 ml medium was added, and cultures were stained with crystal violet after 10 to 14 days.

Real-Time PCR and Stem Cell PCR Array

Total RNA was isolated with TRIZOL Reagent, DNase treated and reverse-transcribed with an optimized blend of the random and oligo (dT) primers (iScript, Bio-Rad). Real-time PCR was performed on iCycler (BioRad) based on SYBR Green I detection. SYBR Green I dye, hot start iTaq DNA polymerase, and buffer mixtures were from BioRad. All quantitations were normalized to internal control genes, including 18s, GAPDH, and Hypoxanthine phosphoribosyltransferase1 expression levels. PCR efficiency was between 90% and 100%. PCR conditions were 95°C for 10 minutes followed by 40 cycles at 95°C for 15 seconds and 60°C at 45 seconds. Melting curves were measured at the end of runs for reaction quality control. Gene specific primers included 5′-CCCAACTTCTTAGAGGGACAAGT-3′ and 5′-CATCACAGACCTGTTATTGCTCA-3′ for 18S; for EPSTI1, 1HPRT1, GAPDH, dnP63, SLUG, TWIST, and fibronectin, see[18,25,23,26,27,28,15], respectively. Stem cell specific markers and stem cell differentiation markers were analyzed by Human Stem Cell PCR Arrays (SABioscience, tetu-bio, Belgium).

Microarray Analysis

The *EPSTI1* gene expression was analyzed in two previously published microarray datasets used to classify breast cancer in five subtypes: normal-like, basal-like, luminal A, luminal B, and ERBB2-positive.[29,30] The two series included gene expression data of 208 experimental samples representing 204 carcinomas and 4 normal breast samples.[29,30] Eight cases were considered unclassifiable in breast cancer subtypes according to a centroid correlation threshold <0.1. The *EPSTI1* gene expression was obtained from

IMAGE clone 1855351. Kruskal–Wallis test was performed using SPSS 15.0 to obtain the *P* value for *EPSTI1* gene expression level in subtypes.

Statistical Analysis

Data are presented as mean ± SEM or ± SD Student paired *t* test was used to determine whether two groups were significantly different. $P < 0.05$ or $P < 0.01$ was considered significant.

Results

EPSTI1 Is a Nucleo-Cytoplasmic Protein Selectively Expressed in Breast Cancer Cells

To find a monospecific antibody against EPSTI1 we screened five different monoclonal and two polyclonal antibodies. Only one polyclonal peptide antibody that we had generated (custom polyclonal; ImmunoVision) and one monoclonal antibody were entirely specific, and only the monoclonal antibody (clone 3G7) reacted equally well in Western blotting and in staining of cells and tissues. Therefore, this antibody was selected for further studies. The specificity of 3G7 was revealed by the appearance of one single band in Western blotting, migrating at the predicted 38 kDa along with the coordinate induction of mRNA and protein in a time course analysis of MDA-MB-231 cells exposed to IFN-α (Figure 1, A–C). This specificity was confirmed by use of four different Stealth RNAi duplexes against EPSTI1, all of which significantly silenced EPSTI1 expression both at the transcriptional and protein level as compared with control RNAi duplexes (Figure 1D). One of the RNAi duplexes, EPSTI1-siRNA2, was particularly efficient, and was together with a control RNAi duplex with a similar CG content, Control-siRNA2, used in subsequent experiments. Immunoperoxidase staining of cells treated with IFN-α was performed, and a characteristic staining pattern was recorded mainly in the nucleus and cytoplasm of the majority of cells (Figure 2A). In the absence of IFN-α, focal staining of breast cancer cells was entirely dependent on coculture with breast fibroblasts (Figure 2B). We have previously shown by use of a tissue panel that relative EPSTI1 expression at the mRNA level is restricted essentially to lymphoid tissue and placenta, while terminally differentiated brain and muscle tissues are devoid of expression.[18] This pattern was confirmed here at the protein level by staining of selected tissue blocks (Figure 2C). Specifically, whereas EPSTI1 stained germinal centers in lymphatic tissue (Figure 2C) and occasional trophoblastic and mesenchymal cells at fetal side of the placenta (not shown), no staining was recorded in muscle (not shown) or brain (Figure 2C). We next examined the staining with EPSTI1 in a series of 25 normal samples from reduction mammoplasties and 40 breast carcinomas. In general the normal biopsies were negative (Figure 3, upper). Occasional staining was seen in stromal cells as well as in the luminal epithelial cells within one ductal profile from two of the biopsies (data not shown).

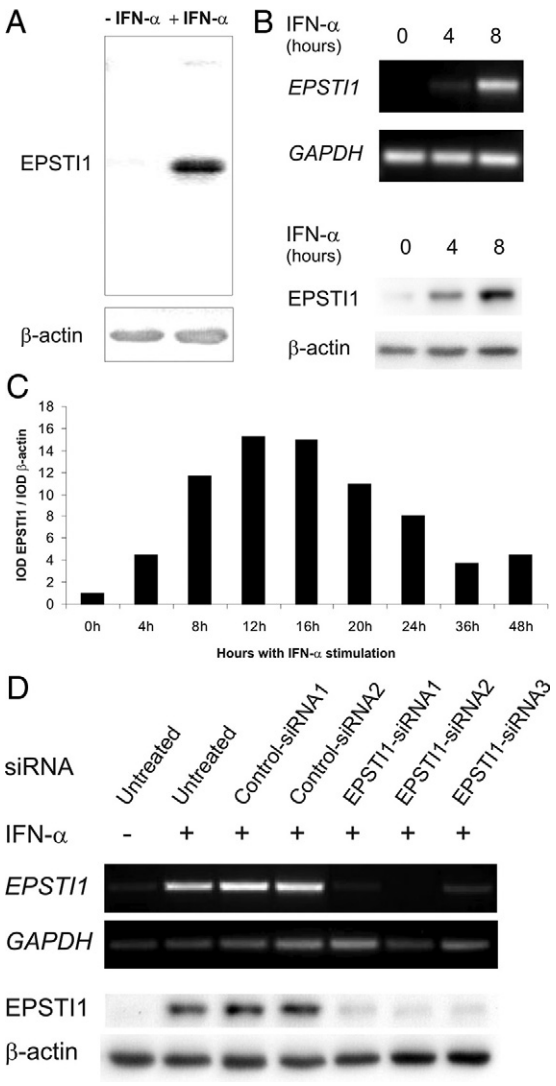

Figure 1. Characterization of the EPSTI1 antibody. **A:** EPSTI1 antibody recognizes a single band at 38 kDa. The human breast cancer cell line MDA-MB-231 was cultured in either the absence (−IFN-α) or in the presence (+IFN-α) of IFN-α for 8 hours before Western blotting. The antibody recognizes a single distinct band (EPSTI1) with a molecular weight of 38 kDa in the lysate of IFN-stimulated cells. Loading was controlled for by staining with β-actin (β-actin). **B:** Coordinate kinetics of EPSTI1 mRNA and protein induction. MDA-MB-231 cells analyzed by RT-PCR (**top panel**) or Western blotting (**lower panel**) after 0, 4, or 8 hours of IFN-α stimulation. Clearly, mRNA and protein are induced with the same kinetics. Loading is controlled for by GAPDH and β-actin (**lower panels**), respectively. **C:** Interferon induction of EPSTI1 protein peaks at 12 hours. Time course of EPSTI1 protein expression in interferon-α–stimulated MDA-MB-231 cells as determined by Western Blotting relative to β-actin expression. The expression level is highest after 12 hours. **D:** The antibody is specific to EPSTI1 as revealed by RNAi. RT-PCR and Western blotting of EPSTI1 in MDA-MB-231 cells without (−) or with (+) induction by IFN-α for 8 hours and without (untreated) or with control RNAi duplexes (control-siRNA1-2) or one of three different RNAi duplexes specific for EPSTI1 (EPSTI1-siRNA1-3). The antibody to EPSTI1 is highly specific because EPSTI1 expression is inhibited at both the transcriptional and translational level. The 38-kDa band essentially disappears on treatment with specific RNA duplexes as compared with the controls.

In contrast, 22 of 40 (55%) breast carcinomas were positive for EPSTI1 defined as a distinct nuclear and/or cytoplasmic staining in foci of cancer cells (Figure 3, middle). That EPSTI1 was a product of tumor-cell fibroblast interaction was further suggested by occasional presence of a gradient of staining with the highest intensity at

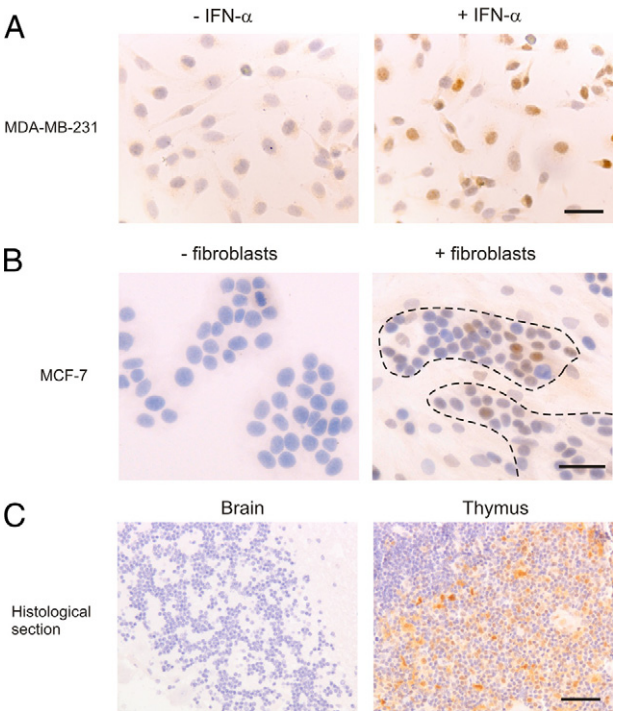

Figure 2. EPSTI1 is a nucleo-cytoplasmic protein. **A:** Interferon-induced EPSTI1 is localized to the nucleus. Immunoperoxidase staining for EPSTI1 in MDA-MB-231 cells either untreated (**left**) or stimulated (**right**) with IFN-α for 19 hours. Staining (brownish) is localized primarily to the nuclei and to a lesser extent to the cytoplasm. Nuclei are counterstained with hematoxylin. (Scale bar = 50 μm). **B:** Fibroblast-induced EPSTI1 is localized to the nuclei of cocultured breast cancer cells. Immunoperoxidase staining for EPSTI1 in MCF-7 cells either alone (**left**) or together (**right**) with fibroblasts. The cancer cell islets are indicated by dotted lines. Staining is seen only among cancer cells in coculture. Nuclei are counterstained with hematoxylin. (Bar = 50 μm). **C:** Staining of histological sections of brain and thymus confirms the specific staining with EPSTI1 *in situ*. Immunoperoxidase staining of sections of human brain (**left**) and human thymus (**right**) with EPSTI1. Staining of nuclei and cytoplasm is seen in thymus only (Scale bar = 50 μm).

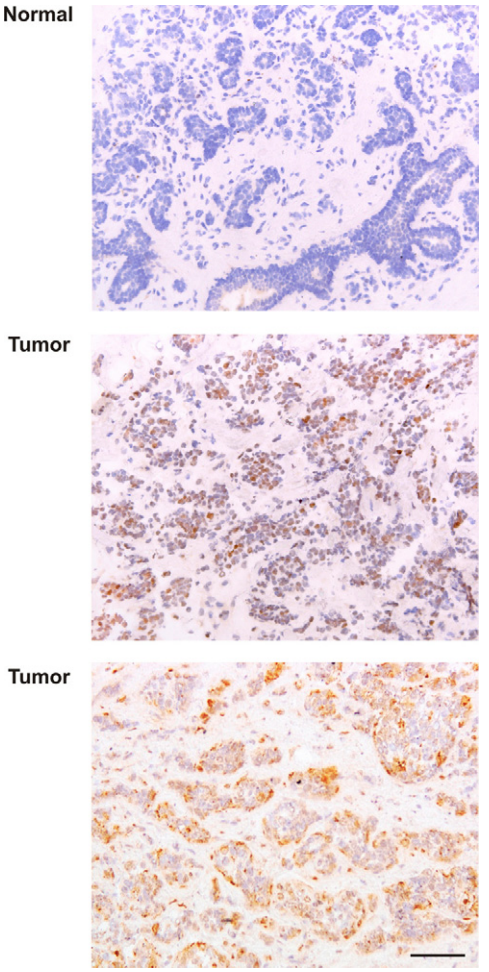

Figure 3. EPSTI1 is a nucleo-cytoplasmic protein in human breast cancer cells. Cryostat sections of (**upper**) a reduction mammoplasty and (**middle**, **lower**) two breast carcinomas stained with immunoperoxidase for EPSTI1. Staining is confined to the nuclei of invading breast cancer cells, and occasionally strong staining is seen at the junction between tumor cell nests and surrounding stroma. Nuclei are counterstained with hematoxylin. (Scale bar = 100 μm).

the epithelial-stromal junction (Figure 3, lower). Furthermore, a putative progenitor function was suspected because staining correlated inversely with the level of differentiation. Thus, among the highly differentiated tubular carcinomas without nuclear pleomorphism, only two of nine (22%) stained with EPSTI1 (Figure 4A, right). To examine whether the carcinomas with the strongest staining belonged to one of the major subtypes we stained with keratin K5, which is a known marker of the basal-like subtype of breast cancer. Interestingly, six of seven (85%) of K5-positive carcinomas stained with EPSTI1 (Figure 4A, left). This subtype is assumed to originate from stem cells or early progenitor cells,[31] and indeed EPSTI1-positive cells were mostly quiescent as revealed by multicolor imaging with EPSTI1 and Ki-67 (Figure 4B). The relation between staining and differentiation was confirmed by analysis of two previously published microarrays datasets used to classify breast cancer in five subtypes: normal-like, basal-like, luminal A, luminal B, and ERBB2-positive.[29,30] Significantly, we found the highest EPSTI1 expression level among the putative stem cell derived (ie, the basal-like and ErbB2$^+$ subtypes[32,33]), and the luminal B subtype, all known to predict for a poor clinical outcome (Figure 4C). This was in contrast to the lower expression of EPSTI1 among the more differentiated subtypes of luminal A and normal-like ($P < 0.001$). In support of a progenitor cell association, EPSTI1 was essentially absent in the normal breast, whereas residual nonmalignant tissue in the vicinity of breast cancer foci showed staining of rare single cells within ductal profiles (Figure 4D). To examine whether these cells belonged to an immature compartment we costained for the luminal epithelial marker progesterone receptor and the myoepithelial marker p63. Clearly, the rare EPSTI1-positive cells were localized in a suprabasal position previously associated with stem cell characteristics[23] including keratin expression (not shown) but without coexpression of any of the differentiated lineage-specific markers (Figure 4D). We therefore conclude that EPSTI1 may delineate a progenitor/stem cell–like population in normal breast, is induced in tumor cells by fibroblast interaction, and associates with breast cancer subtypes with poor prognosis.

EPSTI1 Regulates Tumor Cell Properties

We set out to determine whether expression of EPSTI1 contributes to human breast tumor cell properties. To do

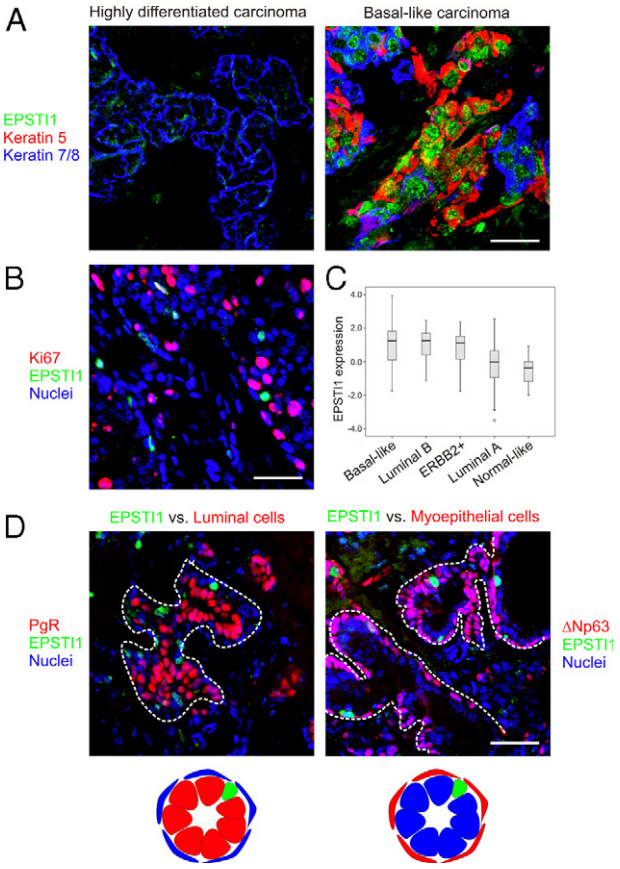

Figure 4. EPSTI1 is expressed in immature breast epithelial cells. **A:** EPSTI1 is highly expressed in basal-like breast cancer. Multicolor confocal imaging of cryostat sections of tubular differentiated human breast cancer without nuclear pleomorphism (**left**) and of basal-like breast cancer (**right**) stained with keratin K7/8 (blue), keratin K5 (red), and EPSTI1 (green). EPSTI1 is highly expressed in the nuclei of the basal-like breast carcinoma. (Scale bar = 50 μm). **B:** EPSTI1 staining correlates with quiescence. Multicolor imaging of human breast cancer stained with EPSTI1 (green), Ki-67 (red), and nuclear stain (blue). Note the segregation of cells staining for EPSTI1 and Ki-67, showing that cells expressing EPSTI1 are not cycling (Scale bar = 50 μm). **C:** EPSTI1 expression is associated with breast cancer subtypes with poor prognosis. Gene expression profiles of 196 breast carcinomas previously obtained using cDNA microarrays. The box plot shows that EPSTI1 expression is significantly higher in breast cancer subtypes with poor prognosis (basal-like, luminal B, and ErbB2+ subtypes) than in those with good prognosis ($P < 0.001$). The dot indicates an outlier. **D:** EPSTI1 expression in residual normal breast tissue is confined to suprabasal epithelial cells. Multicolor confocal imaging of residual normal breast tissue in the vicinity of breast cancer tissue stained for differentiated cells within the luminal epithelial lineage as defined by progesterone receptor (PgR, red, **left**) or within the myoepithelial lineage as defined by p63 (red, **right**), and in both instances costained with EPSTI1 (green) and nucleus counterstain (blue). **Dotted lines** indicate outline of normal epithelial structures. Note that EPSTI1-positive cells neither belong to the luminal nor the myoepithelial lineage as illustrated in the schematic figure in **lower panel** (Scale bar = 50 μm).

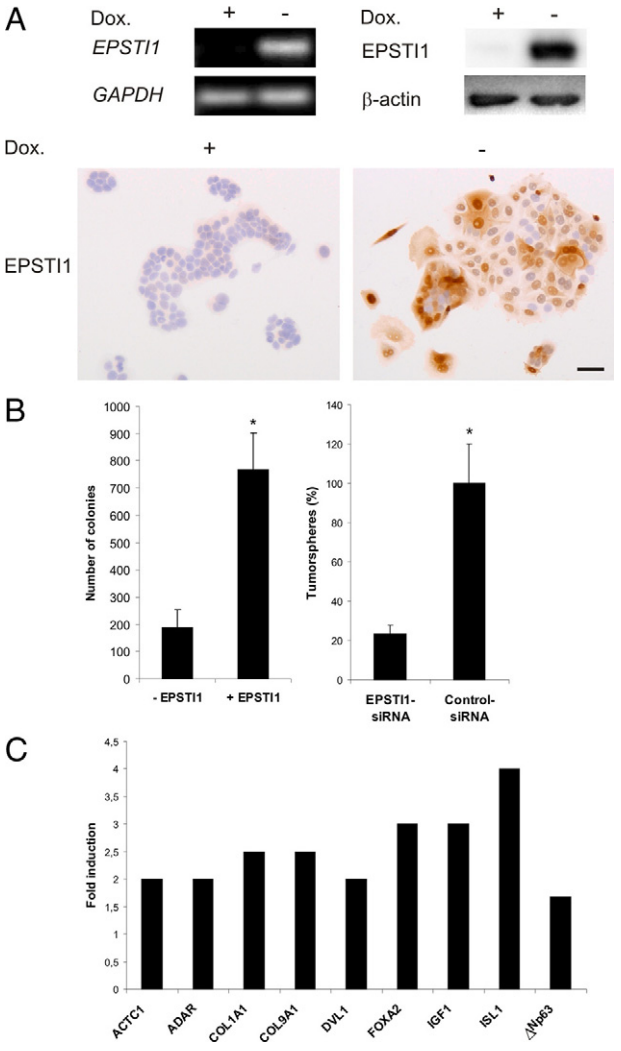

Figure 5. EPSTI1 regulates tumor cell properties. **A:** EPSTI1-transfected MCF-7 cells serve as a model for conditional expression of EPSTI1. RT-PCR (**upper panel**, **left**) and Western blotting (**upper panel**, **right**) of EPSTI1 mRNA and protein, respectively, as regulated by 100 ng/ml doxycycline (Dox. +/−) in a MCF-7–EPSTI1–Tet-off cell line. Note the on/off quality of the expression both at the mRNA and protein level within a time frame of three days. Immunoperoxidase staining (lower panel) showing the typical staining primarily in the nucleus and to a lesser extent in the cytoplasm of the expressing cells (**right**) as compared with doxycycline treated cells (**left**, Scale bar = 50 μm). **B:** EPSTI1 expression facilitates anchorage independent growth in soft agar and tumorsphere formation. **Left:** Bar diagram depicting the quantitative difference in colony forming ability of MCF-7–EPSTI1–Tet-off cells with and without doxycycline. Each bar represents the mean ± SD from triplicate wells (*$P < 0.01$). **Right:** Histogram showing the frequency of single cell–derived tumorspheres from MDA-MB 231 cells induced to express EPSTI1 by IFN-α in the presence of either EPSTI1-siRNA2 (EPSTI1-siRNA) or control-siRNA2 (control-siRNA). A significant difference in favor of EPSTI1 expressing tumorspheres was recorded in both experiments. Each bar represents the mean ± SEM of three experiments performed in duplicate (*$P <$ 0.05). **C:** Stem cell PCR array of MCF-7–EPSTI1–Tet-off cells with and without EPSTI1 expression. Genes associated with embryonic lineage property including ACTC1, FOXA2, ISL1, with mesenchymal cell lineage property markers of COL1A1, and COL9A1, and with a critical Wnt-mediated effector, DVL1 show at least twofold up-regulation. Data are presented as relative expression of genes in EPSTI1-expressing cells, compared with cells without EPSTI1 expression.

so EPSTI1 was stably transduced into MCF-7 cells under the control of the tetracycline-regulated TET-off promoter. Both at the mRNA and protein levels EPSTI1 expression was negligible when cells were treated with doxycycline (Figure 5A). EPSTI1 immunoreactivity in absence of doxycycline was detected in the nuclei and in the cytoplasm (Figure 5A). That EPSTI1 indeed was regulated under these conditions was further confirmed by staining with a monoclonal antibody against the FLAG-tag (data not shown). Nuclear expression of EPSTI1 was most pronounced in subconfluent cultures. Our own studies and those of others have previously demonstrated that the ability to form mammospheres in culture coincides with a stem/progenitor cell phenotype.[24,34] To directly address whether EPSTI1 functions as a potential regulator of breast cancer self-renewal we examined the mammo-

sphere forming ability of MCF-7–EPSTI1–Tet-off cells. We found that the number of single-cell–cloned mammospheres was significantly higher in EPSTI1-expressing cells when compared with those treated with doxycycline (data not shown). That this translated into a more aggressive behavior was confirmed by the soft agar assay where EPSTI1-expressing cells exhibited a fivefold increase in colony forming ability (Figure 5B, left). To confirm a specific role of EPSTI1 in regulation of stem cell properties, we further investigated the effects of siRNA-mediated knockdown of EPSTI1 in a normal-derived breast epithelial cell line with stem cell properties (D492[23]) and in MDA-MB-231, which is a mesenchymal-like breast cancer cell line. In D492 cells, silencing of EPSTI1 caused a significant albeit moderate reduction in mammosphere formation (data not shown). In cancer cells, however, the tumorsphere forming ability was reduced fivefold (Figure 5B, right). This response was further verified *in vivo*. Thus, whereas shEPSTI1 and shControl MDA-MB-231 cells were equally tumorigenic in NOD/SCID mice when inoculated at 5×10^6 and 5×10^5 (two of two inoculations of each), shEPSTI1 completely abolished tumor take when inoculated at 5×10^4 (tumor take in none of six inoculations) as compared with shControl (tumor take in six of eight inoculations). To further explore the possibility that EPSTI1 may regulate stem cell properties in human breast cancer cells we performed a real-time RT-PCR array for stem cell markers in the MCF-7–EPSTI1–Tet-off cells. By this assay EPSTI1 expression led to a more than twofold induction of 9 of 83 putative stem cell markers, whereas none were significantly reduced (Figure 5C), thus suggesting at least a partial induction of a stem cell-like phenotype.

EPSTI1 Substitutes for Fibroblasts in a Tumor-Environment Assay

Evidence has accumulated for the convergence between stem cell properties and epithelial-mesenchymal transition.[15] One of the most fundamental functional consequences of activated fibroblasts on tumor cells is an EMT-like scattering inside a collagen gel as revealed in a tumor environment assay.[3] The coordinate induction of EPSTI1 with spread of tumor cells[18] led us to investigate whether EPSTI1 expression on its own would be enough to substitute for fibroblasts.[3] Accordingly, under standard conditions tumor cells (parent MCF-7 cells) inside a collagen gel formed spherical cell clusters (Figure 6, upper left). However, in the presence of a fibroblast-niche, tumor cells spread and invade the collagen gel forming highly irregular structures ([3]; Figure 6, upper right, 69%). Treatment of parent MCF-7 cells with EPSTI1-siRNA2 before coculture led to a significant reduction in spread (39.8%) as compared with prior treatment with control-siRNA2 (66.7%). Neither growth nor colony size of MCF-7 cultured alone were influenced by this treatment. We next analyzed MCF-7–EPSTI1–Tet-off cells with and without doxycycline in the medium. Remarkably, expression of EPSTI1 led to a more than twofold increase in spread and invasion of tumor cells in a manner very reminiscent of that seen in the presence of fibroblasts (Figure 6, middle and lower panels). Moreover, the observed response could not be further increased by the addition of fibroblasts (data not shown). We conclude that EPSTI1 can substitute for the fibroblast niche in the tumor microenvironment.

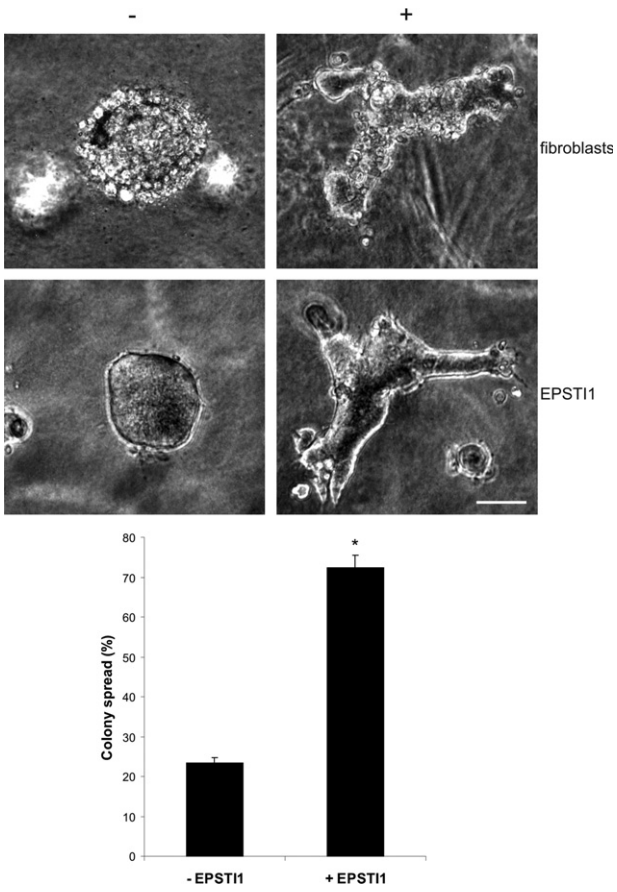

Figure 6. EPSTI1 substitutes for fibroblasts in a tumor environment assay. EPSTI1 expression in MCF-7 cells leads to morphogenesis reminiscent of that obtained by tumor cell-fibroblast interaction. **Upper and middle panels:** Phase contrast micrographs at day 6 of (**upper**) parent MCF-7 cells alone (**left**) or in coculture with fibroblasts (**right**) inside a collagen gel as compared with MCF-7–EPSTI1–Tet-off cells without (**middle panel**, **left**) or with (**middle panel**, **right**) ectopic expression of EPSTI1. Parent MCF-7 cells as well as MCF-7–EPSTI1–Tet-off cells without EPSTI1 expression form typical spherical structures (**upper** and **middle panels**, **left**). Spread and morphogenesis of MCF-7 cells was induced by fibroblasts (**upper panel**, **right**) and a strikingly similar response was observed in MCF-7–EPSTI1–Tet-off cells with ectopic EPSTI1 expression (**middle panel**, **right**). **Lower panel:** Quantification of structure formation by MCF-7–EPSTI1–Tet-off cells within the tumor environment assay as a function of EPSTI1 expression. EPSTI1 expression increases spread and invasion more than twofold. Each bar represents the mean ± SD of three experiments done in triplicate ($^*P < 0.05$). (Scale bar = 50 μm).

EPSTI1 Regulates EMT-Associated Characteristics

To further assess whether EPSTI1 governed a more elaborate EMT process, we introduced MCF-7–EPSTI1–Tet-off cells into monolayer and stained for a number of surrogate EMT markers. On tissue culture plastic expression of EPSTI1 led to the appearance of cells with a mesenchymal morphology as opposed to the cobblestone cell islands in cells treated with doxycycline (Figure 7A). Stem cell–like breast cancers have been reported to be low in claudins.[17] Here, immunofluorescence staining revealed that

EPSTI1 expression correlated with a reduction in Claudin 1 staining and an increased staining with fibronectin (Figure 7B). Also, $\alpha 2\beta 1$-integrin has been shown to correlate with stem cell properties in human prostate epithelial cells and to be a mediator of EMT in human bladder epithelial cells.[35,36] Here we show that expression of EPSTI1 is associated with gain of $\alpha 2\beta 1$ integrin (Figure 7B). This concurred nicely with multicolor imaging of basal-like breast cancer where $\alpha 2\beta 1$ integrin costained with K14/K19 double-positive cells previously identified as stem-like cells in the normal breast ([34]; data not shown). Moreover, RT-PCR analysis showed that mRNAs encoding for mesenchymal markers and EMT-inducing transcription factors SLUG, TWIST, and fibronectin were upregulated (Figure 7C). We next tested whether EPSTI1 in MCF-7–EPSTI1–Tet-off cells could promote EMT-like behavior at the functional level. We therefore performed Boyden-chamber transwell assays and demonstrated that expression of EPSTI1 in MCF7 cells rendered them more migratory (Figure 7D). To confirm a specific role of endogenous EPSTI1 in regulation of stem cell properties and EMT, we further investigated the effects of siRNA-mediated knockdown of EPSTI1 in the mesenchymal-like breast cancer cell line, MDA-MB-231. Silencing of EPSTI1 caused a morphological change toward a more polygonal shape in favor of the more spindle shaped morphology in control cells with control siRNA (Figure 8A). Similarly, MDA-MB-231 cells with EPSTI1-siRNA stained weaker with $\alpha 2\beta 1$-integrin as assessed by immunofluorescence and FACS analysis (Figure 8, B and C) and showed a decline in migratory behavior (Figure 8D).

Collectively, these data provide the first molecular and functional evidence for the involvement of EPSTI1 in a peritumoral niche in human breast cancer. This may add to the understanding of the role and therapeutic potential of the stroma in this disease.

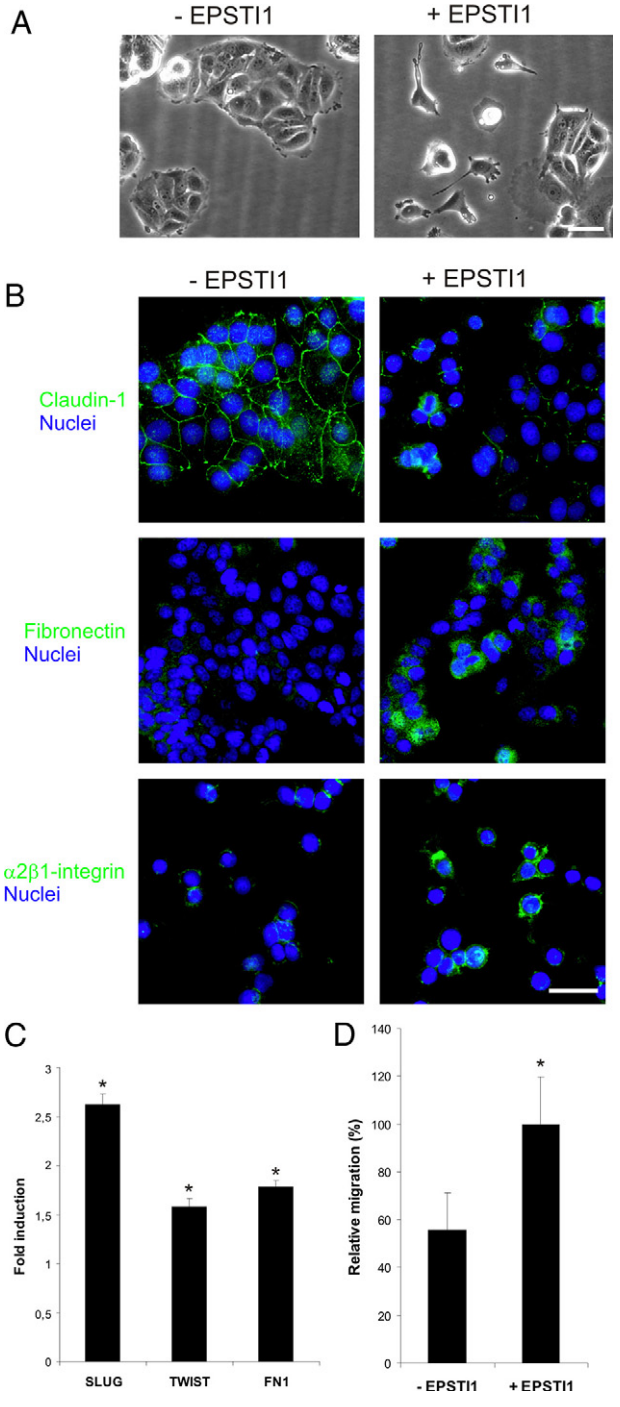

Figure 7. EPSTI1 regulates EMT-associated characteristics. **A:** EPSTI1 expression leads to an EMT morphology. Phase contrast micrographs of MCF-7–TET-off cells without (**left**) and with (**right**) EPSTI1 expression. Note the compact cobblestone morphology without EPSTI1 expression as compared with the spreading migratory morphology with EPSTI1 expression (Bar = 50 μm). **B:** EPSTI1 expression coincides with an EMT-like staining profile. Confocal images of MCF-7–TET-off cells without (**left column**) or with (**right column**) EPSTI1 expression stained for claudin-1 (**upper panel**), fibronectin (**middle panel**), and $\alpha 2\beta 1$-integrin (**lower panel**). EPSTI1 expression is associated with a decline in claudin-1 staining, a stronger staining for fibronectin, and a stronger staining for $\alpha 2\beta 1$ integrin (Scale bar = 50 μm). **C:** EPSTI1 expression correlates with up-regulation of EMT-markers. Quantitative real-time PCR analysis of MCF-7–EPSTI1–Tet-off cells without and with expression of EPSTI1. Note a significant up-regulation of the EMT markers SLUG, TWIST and fibronectin 1 (FN1) on EPSTI1 expression. GAPDH and HRPT1 gene expression were used as controls. The relative quantitative value for each target gene compared with calibrator for the target was expressed as comparative Ct method (2^{-}[Δct-ml] method, Ct and Cc are the mean threshold cycle differences after normalizing to internal control genes). Data represent fold induction of the mean ± SEM (error bar) of three independent experiments done in triplicate (*$P < 0.01$). **D:** EPSTI1 expression increases migratory behavior. Boyden chamber assay for cell migration using the MCF-7–TET-off cells without and with EPSTI1. EPSTI1 expression significantly augments a migratory behavior. Each bar represents the mean ± SEM of three independent experiments in triplicate, *$P < 0.05$.

Discussion

Although it is increasingly well documented that human breast epithelial stem cells and tumor-initiating cells are responsible for maintaining normal and malignant tissues, respectively, it is also well recognized that epithelial cells do not exist independently but function in concert with the stromal microenvironment. Although this intricate interaction indeed is believed to be reciprocal, most of our knowledge pertains to the stromal compartment, the accumulation of myofibroblasts and angiogenesis being the most dramatic consequences of tumor formation.[37,38] Inductive phenomena in epithelia are mostly known from the embryo where mesenchyme provides a gradient,

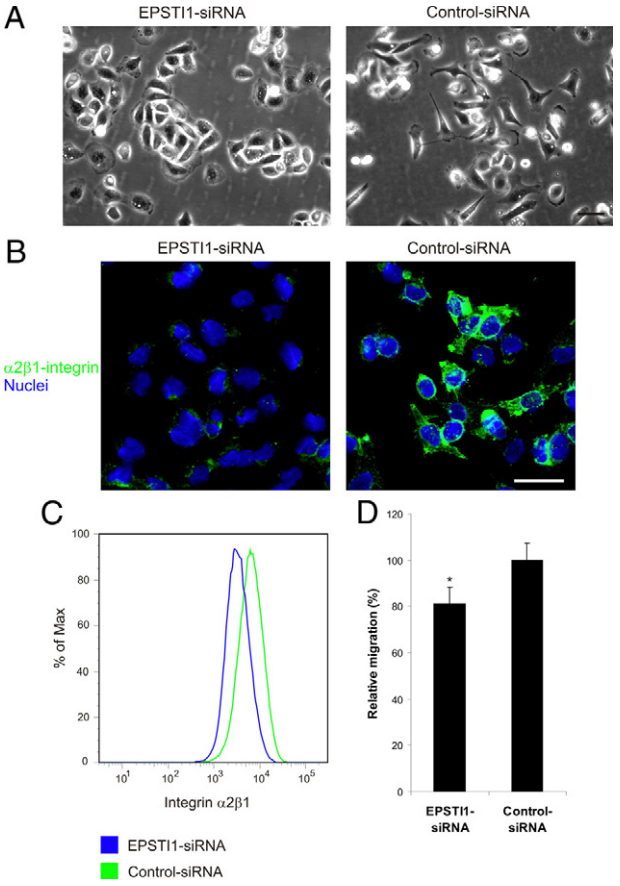

Figure 8. RNAi silencing of EPSTI1 reverses EMT properties. **A:** EPSTI1 silencing leads to a more cuboidal morphology. Phase contrast micrographs of MDA-MB-231 cells transfected with an EPSTI1-specific RNAi duplex, EPSTI1-siRNA2 (left, EPSTI1-siRNA), or a control RNAi duplex, control-siRNA2 (right, Control-siRNA) induced to express EPSTI1 by exposure to IFN-α for 15 hours, followed by trypsination and plating for four hours. Note the spindle-shaped morphology of the EPSTI1-expressing cells compared with the more cuboidal morphology of the EPSTI1-silenced cells. (Scale bar = 50 μm). **B:** Loss of $\alpha2\beta1$-integrin by EPSTI1 silencing. Confocal micrographs of MDA-MB-231 cells treated as in **A**, followed by staining with $\alpha2\beta1$-integrin (green) and nuclear stain (blue). Note the stronger stain of $\alpha2\beta1$-integrin the control (**right**) as compared with cells with silenced EPSTI1 (**left**). (Scale bar = 50 μm). **C:** Loss of $\alpha2\beta1$-integrin at the cell membrane by EPSTI1 silencing. FACS diagram of MDA-MB-231 cells treated as in **A**, followed by staining with $\alpha2\beta1$-integrin, and depicted as EPSTI1-siRNA (blue curve) or Control-siRNA2 (green curve). EPSTI1 silencing correlates with reduction of $\alpha2\beta1$-integrin at the cell surface. **D:** EPSTI1 silencing is inhibitory for cell migration. Boyden chamber assay with MDA-MB-231 cells transfected with an EPSTI1-specific RNAi duplex, EPSTI1-siRNA2 (EPSTI1-siRNA) or a control RNAi duplex, control-siRNA2 (Control-siRNA) induced to express EPSTI1 by exposure to IFN-α for 15 hours before analysis. Silencing of EPSTI1 leads to a less migratory behavior. Each bar represents the mean ± SEM of three independent experiments in triplicate, $^*P < 0.01$.

which determines the fate of multipotent epithelial stem cells.[39] Nevertheless, also within mature connective tissues in adulthood regional differences determine tissue homeostasis such as in skin, prostate, breast, and alimentary tract (for review see[40]). According to this view, the stroma provides a specialized microenvironment referred to as the niche. The niche protects stem cells from inappropriate expansions and directs their critical functions. We provide evidence here supporting an additional, but far less studied, mechanism that governs the phenotype of cancer epithelial cells. Recombinant culture of human breast cancer cells with fibroblasts led to the up-regulation of the IFN response gene *EPSTI1* primarily in the nuclei of tumor cells. *In situ*, EPSTI1 was seen expressed at the epithelial-stromal junction of invading breast cancer. The strongest and most widespread staining was recorded in basal-like putative stem cell–derived tumors. Ectopic expression of EPSTI1 in human breast cancer cells substituted for activated fibroblasts inside a three-dimensional collagen gel leading to autonomous spread of tumor cells within the gels. This was associated with gain of several EMT properties. We propose a novel function for the fibroblast-derived IFN in epithelial–stromal interaction—that of maintaining the tumor cell niche.

We have demonstrated that expression of the IFN response gene EPSTI1 is associated with stem cell–like properties, tumor initiation, and EMT. This is in good agreement with the observation that expression of an IFN response signature including EPSTI1 is associated with a poor prognosis in breast cancer patients and spindloid tumors in mice, which histologically correspond to some of the metaplastic human breast cancers with the most mesenchymal phenotype.[17,20] Thus, the IFN signature accumulates in ER-negative breast cancers including the basal-like presumptive stem cell–derived subtype.[20] Furthermore, our finding that EPSTI1 is expressed in undifferentiated cells with a basal or a suprabasal position in nonmalignant breast tissue adjacent to breast cancer is supported by recent data that mouse mammary gland stem cells (MRU cells) express increased levels of IFN response genes.[41] It is also known that *EPSTI1* is up-regulated along with IFN-α–inducible protein 27 as a consequence of hTERT immortalization of fibroblasts suggesting a role in self-renewal.[42] Nevertheless, our data that EPSTI1-positive cells are mostly quiescent *in situ* based on double-labeling with Ki-67 strongly suggests that the IFN response serves to maintain a reversible pool of proliferation competent quiescent cells. This observation mirrors an observation on mesenchymal stem cells where treatment with neutralizing antibodies to IFN or its receptors resulted in a marked increase in very large colony-forming units from quiescent putative stem cells.[43] It is also supported by recent data from transcriptional profiling of quiescent (Ki-67-negative) human epidermal cells showing an enrichment of IFN response genes in stem cells.[44] We have previously found evidence for a stem cell hierarchy in the human breast with K14/K19 double-positive cells being the earliest detectable cells with stem cell properties.[23,34] Here we found in breast cancer that strong EPSTI1 expression correlates with the presence of K14/K19 double-positive cells. However, whether individual EPSTI1-positive cells indeed represent cancer initiating cells or their immediate progenitor descendants remains to be elucidated. Thus, EPSTI1 is also up-regulated during cell specification of embryonic stem cells into endoderm via mesoderm as induced by inhibition of PI3K.[45] Moreover, in human colon crypts EPSTI1 is expressed in the differentiating upper compartment rather than in the proliferating lower compartment.[46]

The most dramatic consequence of EPSTI1-induction in MCF-7 cells was the autonomous spread and invasion in a three-dimensional collagen lattice. We and others

have previously shown that such invasion is otherwise entirely dependent on direct reciprocal interaction with activated fibroblasts.[3,9,22,47,48] Furthermore, we have shown that the invasion depends to a large degree on fibroblastic deposition of fibronectin, which in turn served as a link between migrating tumor cells and the surrounding collagen scaffold.[22] The presently described substitution of fibroblasts with EPSTI1 in mediating collagen invasion most likely relies on a similar mechanism because fibronectin is induced concurrently with EPSTI1. That fibronectin is up-regulated as part of an EMT program along with SLUG and TWIST, and a number of stem cell properties makes it likely that EPSTI1 feeds in on the newly discovered converging pathways leading to coordinate EMT and stemness in immortalized mammary epithelial cells.[15] The observed EMT program is, however, not complete because the levels of expression of E-cadherin and vimentin remain unaltered. It has been shown though that in a subset of human breast cancer subtypes, EMT is strongly correlated with down-modulation also of claudins.[17] Our finding of a lower claudin-1 staining in EPSTI1-expressing cells is therefore supportive of an, albeit partial, EMT phenotype. Another hallmark of the EMT-phenotype is an increase in cell motility and invasion.[17] Here we found that EPSTI1-positive cells became more migratory. This finding may explain previous findings on pairs of mouse mammary tumors with and without EMT where expression profiling revealed the up-regulation of an IFN signature in the EMT cells.[49] These cells also had activated STAT1, the key signaling pathway in IFN signaling, which is known to contribute to cancer.[48,50] This is particularly interesting in light of the most recent data that an IFN-related gene signature including STAT1 expression is a predictive marker for resistance to chemotherapy and radiation in human breast cancer.[51] These and our data may further support the converging EMT and stem cell pathways because drug resistance has been shown to lead to the enlargement of the stem cell compartment in tumors (for review see[52]).

The connections described above for human breast cancer point to the peritumoral stroma (ie, the [myo]fibroblasts as a niche for breast cancer stem cells). This means that the CSCs accumulate at the tumor cell nest-stroma junction under maximal influence of adjacent myofibroblasts. This also means that although IFN may have a role in treatment of cancer mainly in reducing angiogenesis,[53] it may also have adverse effects in supporting survival of CSCs maybe even under hypoxic conditions.

Acknowledgments

We thank Søllerød Privathospital and the Private Clinic for providing the normal breast biopsy material. We also thank Tove Marianne Lund, Mimi Birkelund, Lena Kristensen, and Margit Bæksted for expert technical assistance.

References

1. Rønnov-Jessen L, Bissell MJ: Breast cancer by proxy: can the microenvironment be both the cause and consequence? Trends Mol Med 2009, 15:5–13
2. Sappino A-P, Skalli O, Jackson B, Schürch W, Gabbiani G: Smooth-muscle differentiation in stromal cells of malignant and non-malignant breast tissues. Int J Cancer 1988, 41:707–712
3. Rønnov-Jessen L, Petersen OW, Koteliansky VE, Bissell MJ: The origin of the myofibroblasts in breast cancer: recapitulation of tumor environment in culture unravels diversity and implicates converted fibroblasts and recruited smooth muscle cells. J Clin Invest 1995, 95:859–873
4. Orimo A, Gupta PB, Sgroi DC, Arenzana-Seisdedos F, Delaunay T, Naeem R, Carey VJ, Richardson AL, Weinberg RA: Stromal fibroblasts present in invasive human breast carcinomas promote tumor growth and angiogenesis through elevated SDF-1/CXCL12 secretion. Cell 2005, 121:335–348
5. Schor SL, Ellis IR, Jones SJ, Baillie R, Seneviratne K, Clausen J, Motegi K, Vojtesek B, Kankova K, Furrie E, Sales MJ, Schor AM, Kay RA: Migration-stimulating factor: a genetically truncated onco-fetal fibronectin isoform expressed by carcinoma and tumor-associated stromal cells. Cancer Res 2003, 63:8827–8836
6. De Wever O, Nguyen QD, Van Hoorde L, Bracke M, Bruyneel E, Gespach C, Mareel M: Tenascin-C and SF/HGF produced by myofibroblasts in vitro provide convergent pro-invasive signals to human colon cancer cells through RhoA and Rac. FASEB J 2004, 18:1016–1018
7. Schnack Nielsen B, Sehested M, Timshel S, Pyke C, Danø K: Messenger RNA for urokinase plasminogen activator (uPA) is expressed in myofibroblasts adjacent to cancer cells in human breast cancer. Lab Invest 1996, 74:168–177
8. Lin EY, Pollard JW: Tumor-associated macrophages press the angiogenic switch in breast cancer. Cancer Res 2007, 67:5064–5066
9. Kankuri E, Cholujova D, Comajova M, Vaheri A, Bizik J: Induction of hepatocyte growth factor/scatter factor by fibroblast clustering directly promotes tumor cell invasiveness. Cancer Res 2005, 65: 9914–9922
10. Stoker M, Gherardi E, Perryman M, Gray J: Scatter factor is a fibroblast-derived modulator of epithelial cell mobility. Nature 1987, 327:239–242
11. Montesano R, Matsumoto K, Nakamura T, Orci L: Identification of a fibroblast-derived epithelial morphogen as hepatocyte growth factor. Cell 1991, 67:901–908
12. Savagner P, Yamada KM, Thiery JP: The zinc-finger protein slug causes desmosome dissociation, an initial and necessary step for growth factor-induced epithelial-mesenchymal transition. J Cell Biol 1997, 137:1403–1419
13. Thiery JP, Chopin D: Epithelial cell plasticity in development and tumor progression. Cancer Metastasis Rev 1999, 18:31–42
14. Petersen OW, Nielsen HL, Gudjonsson T, Villadsen R, Rønnov-Jessen L, Bissell MJ: The plasticity of human breast carcinoma cells is more than epithelial to mesenchymal conversion. Breast Cancer Res 2001, 3:213–217
15. Mani SA, Guo W, Liao MJ, Eaton EN, Ayyanan A, Zhou AY, Brooks M, Reinhard F, Zhang CC, Shipitsin M, Campbell LL, Polyak K, Brisken C, Yang J, Weinberg RA: The epithelial-mesenchymal transition generates cells with properties of stem cells. Cell 2008, 133:704–715
16. Morel AP, Lievre M, Thomas C, Hinkal G, Ansieau S, Puisieux A: Generation of breast cancer stem cells through epithelial-mesenchymal transition. PLoS ONE 2008, 3:e2888
17. Herschkowitz JI, Simin K, Weigman VJ, Mikaelian I, Usary J, Hu Z, Rasmussen KE, Jones LP, Assefnia S, Chandrasekharan S, Backlund MG, Yin Y, Khramtsov AI, Bastein R, Quackenbush J, Glazer RI, Brown PH, Green JE, Kopelovich L, Furth PA, Palazzo JP, Olopade OI, Bernard PS, Churchill GA, Van Dyke T, Perou CM: Identification of conserved gene expression features between murine mammary carcinoma models and human breast tumors. Genome Biol 2007, 8:R76
18. Nielsen HL, Rønnov-Jessen L, Villadsen R, Petersen OW: Identification of EPSTI1, a novel gene induced by epithelial-stromal interaction in human breast cancer. Genomics 2002, 79:703–710
19. Ishii T, Onda H, Tanigawa A, Ohshima S, Fujiwara H, Mima T, Katada Y, Deguchi H, Suemura M, Miyake T, Miyatake K, Kawase I, Zhao H, Tomiyama Y, Saeki Y, Nojima H: Isolation and expression profiling of

genes upregulated in the peripheral blood cells of systemic lupus erythematosus patients. DNA Res 2005, 12:429–439
20. Buess M, Nuyten DS, Hastie T, Nielsen T, Pesich R, Brown PO: Characterization of heterotypic interaction effects in vitro to deconvolute global gene expression profiles in cancer. Genome Biol 2007, 8:R191
21. Rønnov-Jessen L, van Deurs B, Celis JE, Petersen OW: Smooth muscle differentiation in cultured human breast gland stromal cells. Lab Invest 1990, 63:532–543
22. Rønnov-Jessen L, van Deurs B, Nielsen M, Petersen OW: Identification, paracrine generation and possible function of human breast carcinoma myofibroblasts in culture. In Vitro Cell Dev Biol 1992, 28A:273–283
23. Gudjonsson T, Villadsen R, Nielsen HL, Ronnov-Jessen L, Bissell MJ, Petersen OW: Isolation, immortalization, and characterization of a human breast epithelial cell line with stem cell properties. Genes Dev 2002, 16:693–706
24. Dontu G, Abdallah WM, Foley JM, Jackson KW, Clarke MF, Kawamura MJ, Wicha MS: In vitro propagation and transcriptional profiling of human mammary stem/progenitor cells. Genes Dev 2003, 17:1253–1270
25. Trollmann R, Schoof E, Beinder E, Wenzel D, Rascher W, Dotsch J: Adrenomedullin gene expression in human placental tIssue and leukocytes: a potential marker of severe tIssue hypoxia in neonates with birth asphyxia. Eur J Endocrinol 2002, 147:711–716
26. Kumamoto H, Ohki K, Ooya K: Expression of p63 and p73 in ameloblastomas. J Oral Pathol Med 2005, 34:220–226
27. Storci G, Sansone P, Trere D, Tavolari S, Taffurelli M, Ceccarelli C, Guarnieri T, Paterini P, Pariali M, Montanaro L, Santini D, Chieco P, Bonafé M: The basal-like breast carcinoma phenotype is regulated by SLUG gene expression. J Pathol 2008, 214:25–37
28. Yang J, Mani SA, Donaher JL, Ramaswamy S, Itzykson RA, Come C, Savagner P, Gitelman I, Richardson A, Weinberg RA: Twist, a master regulator of morphogenesis, plays an essential role in tumor metastasis. Cell 2004, 117:927–939
29. Naume B, Zhao X, Synnetvedt M, Borgen E, Russnes HG, Lingjærde OC, Strømberg M, Wiedswang G, Kvalheim G, Kåresen R, Nesland JM, Børresen-Dale A-L, Sørlie T: Presence of bone marrow micrometastasis is associated with different recurrence risk within molecular subtypes of breast cancer. Mol Oncol 2007, 1:160–171
30. Langerød A, Zhao H, Borgan Ø, Nesland JM, Bukholm IRK, Ikdahl T, Kåresen R, Børresen-Dale A-L, Jeffrey SS: TP53 mutation status and gene expression profiles are powerful prognostoc markers of breast cancer. Breast Cancer Res 2007, 9:R30
31. Bocker W, Moll R, Poremba C, Holland R, Van Diest PJ, Dervan P, Burger H, Wai D, Ina Diallo R, Brandt B, Herbst H, Schmidt A, Lerch MM, Buchwallow IB: Common adult stem cells in the human breast give rise to glandular and myoepithelial cell lineages: a new cell biological concept. Lab Invest 2002, 82:737–746
32. Korkaya H, Paulson A, Iovino F, Wicha MS: HER2 regulates the mammary stem/progenitor cell population driving tumorigenesis and invasion. Oncogene 2008, 27:6120–6130
33. Liu S, Ginestier C, Charafe-Jauffret E, Foco H, Kleer CG, Merajver SD, Dontu G, Wicha MS: BRCA1 regulates human mammary stem/progenitor cell fate. Proc Natl Acad Sci USA 2008, 105:1680–1685
34. Villadsen R, Fridriksdottir AJ, Rønnov-Jessen L, Gudjonsson T, Rank F, Labarge MA, Bissell MJ, Petersen OW: Evidence for a stem cell hiearachy in the adult human breast. J Cell Biol 2007, 177:87–101
35. Valles AM, Boyer B, Tarone G, Thiery JP: Alpha 2 beta 1 integrin is required for the collagen and FGF-1 induced cell dispersion in a rat bladder carcinoma cell line. Cell Adhes Commun 1996, 4:187–199
36. Heer R, Collins AT, Robson CN, Shenton BK, Leung HY: KGF suppresses alpha2beta1 integrin function and promotes differentiation of the transient amplifying population in human prostatic epithelium. J Cell Sci 2006, 119:1416–1424
37. Rønnov-Jessen L, Petersen OW, Bissell MJ: Cellular changes involved in conversion of normal to malignant breast: the importance of the stromal reaction. Physiol Rev 1996, 76:69–125
38. Folkman J: Angiogenesis and breast cancer. J Clin Oncol 1994, 12:441–443
39. Veltmaat JM, Relaix F, Le LT, Kratochwil K, Sala FG, van Veelen W, Rice R, Spencer-Dene B, Mailleux AA, Rice DP, Thiery JP, Bellusci S: Gli3-mediated somitic Fgf10 expression gradients are required for the induction and patterning of mammary epithelium along the embryonic axes. Development 2006, 133:2325–2335
40. Fuchs E, Tumbar T, Guasch G: Socializing with the neighbors: stem cells and their niche. Cell 2004, 116:769–778
41. Shackleton M, Vaillant F, Simpson KJ, Stingl J, Smyth GK, Asselin-Labat ML, Wu L, Lindeman GJ, Visvader JE: Generation of a functional mammary gland from a single stem cell. Nature 2006, 439:84–88
42. Hiyama K, Tanimoto K, Nishimura Y, Tsugane M, Fukuba I, Sotomaru Y, Hiyama E, Nishiyama M: Exploration of the genes responsible for unlimited proliferation of immortalized lung fibroblasts. Exp Lung Res 2008, 34:373–390
43. Peiffer I, Eid P, Barbet R, Li ML, Oostendorp RA, Haydont V, Monier MN, Milon L, Fortunel N, Charbord P, Tovey M, Hatzfeld J, Hatzfeld A: A sub-population of high proliferative potential-quiescent human mesenchymal stem cells is under the reversible control of interferon alpha/beta. Leukemia 2007, 21:714–724
44. Kocer SS, Djuric PM, Bugallo MF, Simon SR, Matic M: Transcriptional profiling of putative human epithelial stem cells. BMC Genomics 2008, 9:359–373
45. McLean AB, D'Amour KA, Jones KL, Krishnamoorthy M, Kulik MJ, Reynolds DM, Sheppard AM, Liu H, Xu Y, Baetge EE, Dalton S: Activin a efficiently specifies definitive endoderm from human embryonic stem cells only when phosphatidylinositol 3-kinase signaling is suppressed. Stem Cells 2007, 25:29–38
46. Kosinski C, Li VS, Chan AS, Zhang J, Ho C, Tsui WY, Chan TL, Mifflin RC, Powell DW, Yuen ST, Leung SY, Chen X: Gene expression patterns of human colon tops and basal crypts and BMP antagonists as intestinal stem cell niche factors. Proc Natl Acad Sci USA 2007, 104:15418–15423
47. Petersen OW, Nielsen HL, Gudjonsson T, Villadsen R, Rank F, Niebuhr E, Bissell MJ, Rønnov-Jessen L: Epithelial to mesenchymal transition in human breast cancer can provide a non-malignant stroma. Am J Pathol 2003, 162:391–402
48. Jechlinger M, Sommer A, Moriggl R, Seither P, Kraut N, Capodiecci P, Donovan M, Cordon-Cardo C, Beug H, Grunert S: Autocrine PDGFR signaling promotes mammary cancer metastasis. J Clin Invest 2006, 116:1561–1570
49. Jechlinger M, Grunert S, Tamir IH, Janda E, Ludemann S, Waerner T, Seither P, Weith A, Beug H, Kraut N: Expression profiling of epithelial plasticity in tumor progression. Oncogene 2003, 22:7155–7169
50. Kovacic B, Stoiber D, Moriggl R, Weisz E, Ott RG, Kreibich R, Levy DE, Beug H, Freissmuth M, Sexl V: STAT1 acts as a tumor promoter for leukemia development. Cancer Cell 2006, 10:77–87
51. Weichselbaum RR, Ishwaran H, Yoon T, Nuyten DS, Baker SW, Khodarev N, Su AW, Shaikh AY, Roach P, Kreike B, Roizman B, Bergh J, Pawitan Y, van de Vijver MJ, Minn AJ: An interferon-related gene signature for DNA damage resistance is a predictive marker for chemotherapy and radiation for breast cancer. Proc Natl Acad Sci USA 2008, 105:18490–18495
52. Eyler CE, Rich JN: Survival of the fittest: cancer stem cells in therapeutic resistance and angiogenesis. J Clin Oncol 2008, 26:2839–2845
53. Krop I, Marz A, Carlsson H, Li X, Bloushtain-Qimron N, Hu M, Gelman R, Sabel MS, Schnitt S, Ramaswamy S, Kleer CG, Enerback C, Polyak K: A putative role for psoriasin in breast tumor progression. Cancer Res 2005, 65:11326–11334